IMPLEMENTATION OF A MULTIFONCTIONNAL PIEZOELECTRIC EMBEDDED SENSOR FOR THE HEALTH MONITORING OF THE WHOLE LIFE CYCLE OF A REAL COMPOSITE STRUCTURE

Monnier T., Guy P., Godin N., Jayet Y.

GEMPPM –INSA de Lyon, 7 avenue Jean Capelle, 69621-Villeurbanne - France

ABSTRACT

The lifetime and the health condition of a composite structure is closely linked to both the homogeneously distribution evolution of its mechanical properties during its life cycle (curing and ageing) and the degradation associated to the presence of localised defects such as matrix or fibre cracks or delamination.

Piezoelectric ceramic can be used as "passive" sensors to sense the strain or stress waves which travel into the material and are associated to the initiation of damage (acoustic emission) or as "active" sensors to generate ultrasonic waves for non destructive evaluation purposes. In the active mode, the axial vibration modes are used to generate bulk compressional or shear waves while the radial vibration modes are used in order to generate guided Lamb waves. Those ultrasonic elastic waves are sensitive to the viscolelastic properties and the presence of defects inside the structure.

In this paper, we present experimental results obtained on structures instrumented with of several piezoelectric PZT discs.

The evolution of the electrical impedance of such active elements with frequency is computed thanks to a one-dimensional model. It can be related to the physical and geometrical properties and to the acoustical characteristics (velocity and attenuation of plane waves) of the surrounding media. It is therefore possible by solving the inverse problem to extract the attenuation and velocity. This technique is applied to monitor the whole curing process of polymer composites. Since the piezoelectric implants remain inserted in the structure they are used to monitor the microstructural evolution during the whole lifetime of the composite structure.

A second application of these piezoelectric PZT embedded elements concerns the local defect detection. These elements have been arranged in a pitch-catch configuration in order to monitor localised damages which can arise in the composite structure. The dimensions of the piezoelectric elements are determined in order to uncouple the axial and radial vibration modes. So in the low frequency range, a particular Lamb mode (either symmetrical or anti symmetrical) can be preferably generated by tuning the frequency of the applied voltage. The experimental results obtained on a damaged composite structure, will be compared to those acquired on a sane one. These comparisons will be commented and interpreted by means of finite element modelling of the interaction of the wave with a delamination.

Finally the piezoelectric PZT discs are used as passive sensors in the classical Acoustic Emission setup. The structure is stressed and the strain energy released by the appearance of damage results in stress waves propagation. The signal delivered by the embedded sensor can be considered as the acoustic signature of the different damage modes. Using combinations of acoustic emission amplitude distribution and neural networks (Kohonen self organising maps) enables to discriminate signals originating from different damage sources.

The interest of such a multifunctional *in situ* device lies in the fact that it provides complementary information about the microstructure evolution of the propagating medium (e.g. to its health condition) during all its life cycle. While, the high frequency vibration related to the electrical impedance is significant of the curing conditions and ageing, the low frequency Lamb waves are used for localised damages detection. Finally, the waveforms due to the Acoustic Emission of the stressed structure allow us to determine the location and the nature of active damages. These interrelated studies are supported by different analytical or numerical modelling or signal processing software developed especially for this purpose in our laboratory.

These results in the scope of smart materials constitute a very important tool for the challenging topics of real material and structure health monitoring and residual lifetime prediction.

1. INTRODUCTION

The damage detection and characterisation of complex industrial structures are conventionally performed through classical Non Destructive Evaluation (NDE) techniques such as tap testing, visual inspection, ultrasonics, eddy currents, flux leakage, thermography, liquid penetrant, acoustic emission, X-Rays inspection, and so on. The cost of these maintenance procedures results from the direct hardware and manpower cost but also from the resulting lost of exploitation. One of the possible options to reduce this cost is the utilisation of in-situ and continuous Structural Health Monitoring (SHM). The future on-line monitoring systems

should be small-sized in order to minimise the damage initiation risk, they might have a good sensitivity and robustness. This approach is part of the more general concept so called "smart materials and structures". Actually, if sensors are embedded in a composite structure before curing in order to monitor and optimise its processing parameters, they are able, since they remain in the structure, to assume the health monitoring function in the second stage of the structure lifetime. Furthermore, in slightly damaged systems, it becomes reasonable to use the collected data for an on-line tentative prediction of the residual lifetime.
In that context some authors [1] recently underlined the increasing need of reliable on-line devices for SHM.
The health state to be evaluated depends on the homogeneously distributed degradation of its mechanical properties during its life cycle (ageing) as well as on the initiation and growth of localised damages such as cracks or delaminations. The requested techniques have to be able to recover quantitative information about both phenomenon.
The piezoelectric insert, health monitoring technique can be a good option since it allows recovering both kinds of information [2-5].

2.CURING PROCESS AND AGEING MONITORING OF COMPOSITES

When the frequency of the applied voltage is within the frequency range of the thickness vibration mode of the sensor, a bulk wave propagates forward and backward through the thickness of the host structure and interacts with the piezoelectric element. The evolution of the sensor's impedance with frequency can be measured and related to the mechanical and physical properties of both the surrounding media and the sensor itself.[2, 3]. The properties measured by this method are concerned with a limited volume in the close vicinity of the sensor. Nevertheless, if the ageing of the composite structure is assumed to be homogeneous, the in-service monitoring of the impedance is representative of the whole material degradation. This method can appear very similar to the Electro Mechanical Impedance (E/M) method described by Giurgiutiu, but it is different. The E/M method acts in the low frequency range and relates the real part of the sensor's impedance to the mechanical impedance of the tested. In the present case, the impedance is only sensitive to the viscoelastic properties of the material in the vicinity of the sensor.
A simple analytic model [2,3] shows that the impedance of this element depends on the physical properties of the element itself as well as on the acoustical properties of the surrounding medium. The acoustical parameters, namely the velocity and the attenuation are directly linked to the elastic properties and microstructure of the materials. Then for NDE purposes, the resolution of the so-called inverse problem allows to recover the ultrasonic properties of the surrounding plates from the measurement of the electric impedance of the piezoelectric sensor.
The piezoelectric ceramic considered here is a disk of negligible thickness in regard with its diameter so that, the radial and thickness vibration modes will occur in two very different frequency ranges and they will be considered as independent one from the other.
So only the thickness mode of vibration will be taken into account and consequently a 1D approach is convenient to model the frequency evolution of the impedance in relation with the axial vibration modes. A schematic of the problem is presented in Fig.1. The active element of thickness e is considered to be of infinite lateral dimensions. It is coupled to two different viscoelastic media (subscripts 2 and 3 respectively) of thicknesses e_2 and e_3. Those two media are themselves coupled to two semi-infinite media (subscripts *1* and *4*).

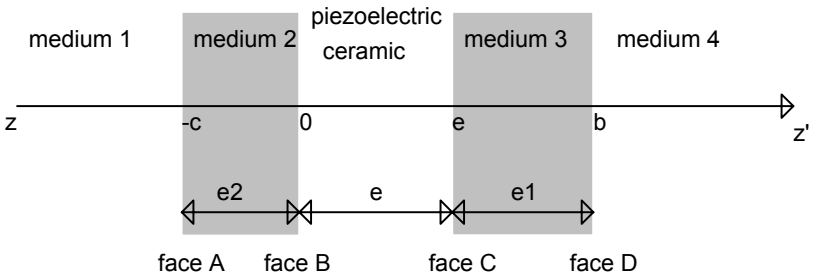

Fig. 1, Schematic of the one dimensional model

Our model derives the impedance analytical expression from the piezoelectricity equations taking into account the wave propagation. It is found [2] that whatever the frequency, the impedance of the piezoelectric element depends on the piezoelectric, viscoelastic and geometrical parameters of both the ceramic and the surrounding media.
Provided the properties of each material the model can be experimentally validated by comparison of the simulated results with experimental measurements of the electric impedance of the active element [3] as done in the following example.
A PZT5 ceramic is bounded in between two PMMA layers of different thickness (5.95 mm and 18.64 mm respectively). The whole structure is placed in air, so that the acoustical properties of the media 1 and 4 are those of air.
The measurements are realized with the help of an HP 4194A impedancemeter. Fig 2 presents a comparison of the measured and simulated modulus of the electric impedance as a function of frequency.

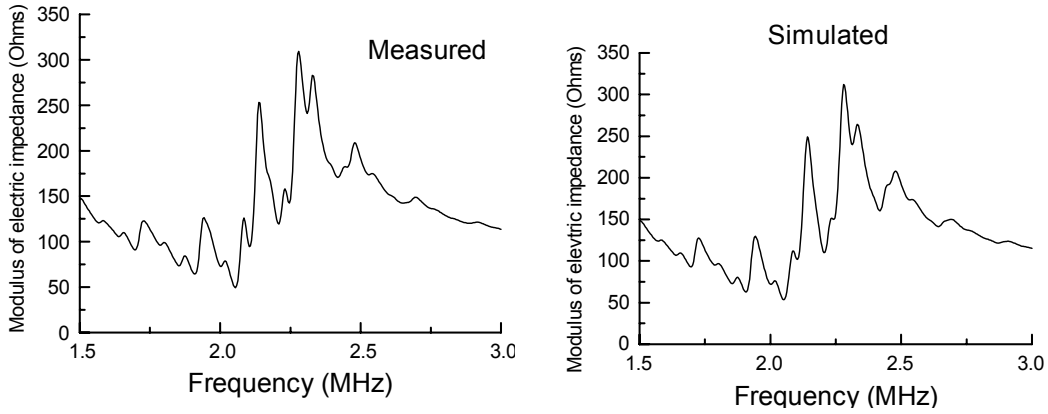

Fig. 2:, Measured and simulated spectra. Ceramic between two PMMA plates of 5.95 mm and 18.64 mm

An excellent agreement has been found between simulated and measured impedances. Then the model can be considered as valid for that kind of experimentation and that it may be used to solve the inverse problem which consists in determining the acoustical properties of the materials surrounding the active element from an electric impedance measurement.
The numerical process that has been used is based on a non linear optimization algorithm. From experimental data the program seeks for the parameters that make the calculated results converge to the experimental ones.
The surrounding media to be characterized are a 3.04 mm layer of PMMA on one side and a 2.24 mm thick layer of PA (polyamide, semi-crystalline polymer)
By application of the optimization algorithm, the dispersion laws for the acoustic velocity and attenuation have been determined in a frequency range extending from 1.5 MHz to 3 MHz. These results obtained from the measured impedance are compared with those determined by classical ultrasonic spectroscopy.
Again, an excellent agreement can be found between these results presented in Fig. 3.

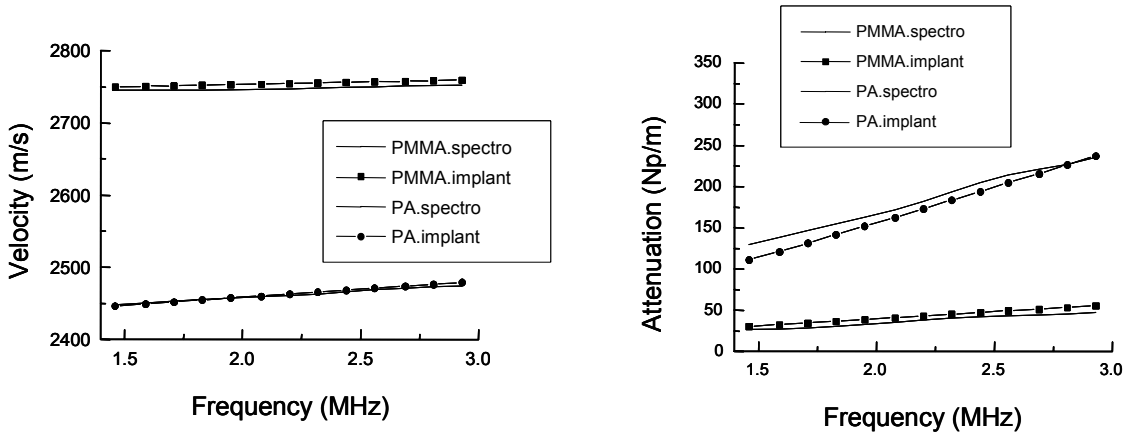

Fig. 3, Impedance measurement compared with spectroscopy results on PMMA and PA.

It has to be noted that although velocity and attenuation are extracted separately from the model, they are actually linked by the Kramers-Kronig laws which ensure the causality of the acoustical waveforms. This enables the user to check the reliability of the recovered properties [3, 6].

The method described in the previous section is applied to monitor the curing of any polymer-based composite. The following results have been obtained on an epoxy resin reinforced with 57% w glass fibers submitted to a well-defined temperature cycle. Impedance curves are recorded as a function of the curing time. So, the attenuation and the velocity can be calculated at different polymerisation ratios.

The acoustical parameters of the composite extracted from the impedance measurement of such a piezoelectric element are represented in the Fig. 4 as a function of the polymerisation time. The considered acoustical parameters are the velocity and the attenuation magnitudes at 2 MHz frequency (resonance frequency of the ceramic plate).

These results show that the velocity increases during the cure indicating that the mechanical modulus becomes greater. As for the attenuation, it decreases during polymerisation indicating that the viscosity of the resin becomes lower and lower.

The physical processes associated to the polymerization process can be monitored and controlled.

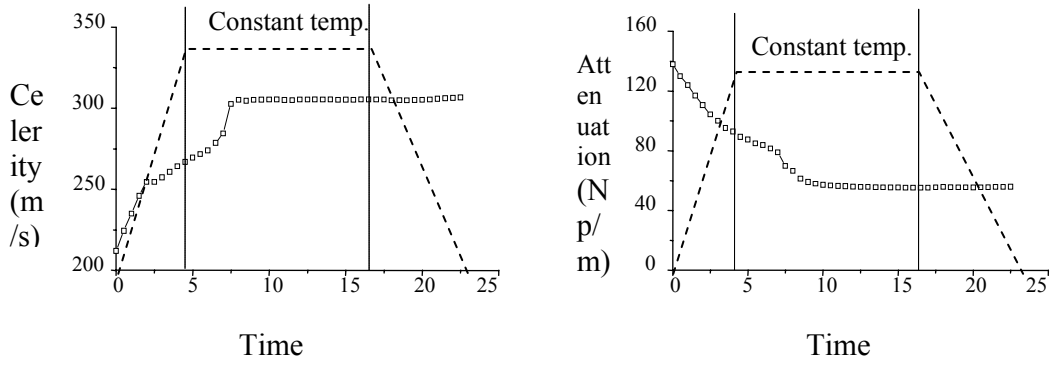

Fig. 4, Curing process monitoring by impedance measurement

3.ACTIVE DAMAGE DETECTION IN COMPOSITE STRUCTURES

The following results have been obtained on a 6mm-thick Carbon Fibres Reinforced Plastic (CFRP) plate of dimension 255 x 300 mm2 and made-up of 22 carbon/epoxy uni-directional plies stacked according to the sequence $[45°,[-45°_2,45°_2]_{10},135°]$ where 0° and 90° denote the directions of the plate edges.

The knowledge of the various Lamb modes properties is essential to identify the components of the transmitted waveforms, to help data interpretation, to assess the different mode sensitivity to different kinds of defects, and also to locate defects. This requires the measurement of the material densities and stiffness tensors. The elastic modulii were measured using an ultrasonic technique available in our laboratory.

To introduce realistic damages we used a drop-weight calibrated impacting device, which can record the time-history of the load and displacement of a 20 - mm diameter hemispherical impactor. As the impacts were controlled in a very reproducible way, it has been determined that the damaging threshold of the composite plate was between 6.13 and 6.38 joules.

Then a sample plate has been submitted to four successive impacts of energy 2, 4, 8 and 8 joules at the same location.

After each impact the sample was interrogated with propagating Lamb modes. This consisted in exciting the sensor with a tone burst of adjustable frequency, in order to select a particular Lamb mode (A_0 or S_0), and in recording the transmitted waveforms on the receiver. It is difficult to find a reliable discriminating parameter through the observation of the time signals. Hence, it was decided to use spectral analysis. Fast Fourier Transform for each waveform was computed, and to take into account the dispersion of the results, a set of one hundred raw reference signatures was recorded in the sane plate, and ten raw signatures were recorded after each impact.

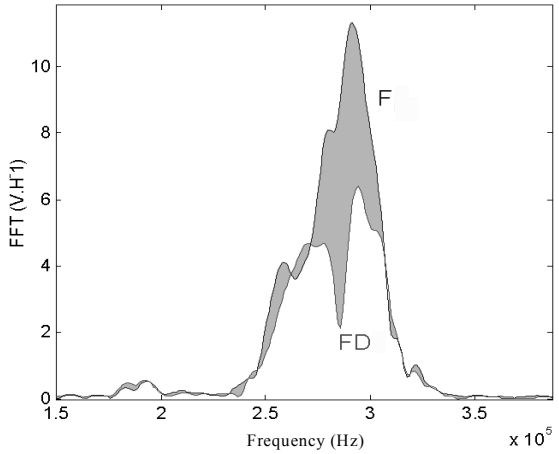

Fig. 5, Transmitted frequency spectrum of the undamaged (F) compared to the frequency spectrum of the damaged (FD) CFRP plate for S_0 mode.

We proposed to introduce a number we called damage index *DI*, defined as follows :

$$DI = \frac{\sum_{i=1}^{n} |F_i - FD_i|}{\sum_{i=1}^{n} |F_i|}.$$

We first chose a reference signal. The waveform is numerically windowed and the corresponding spectrum *F* is computed. *DI* represents the cumulated absolute value of the difference between this reference and the sample spectra *FD* calculated for each frequency

point *i*. This quantity is normalized to the absolute value of the reference spectrum. In other words *DI* is the grayed area in Fig. 5, divided by the reference spectrum area. So *DI* = 0 when the measured spectrum is identical to the reference one, and *DI* = 1 when the damaged spectrum is null. This occurs when no signal can propagate between the emitter and the receiver (the plate is totally broken).

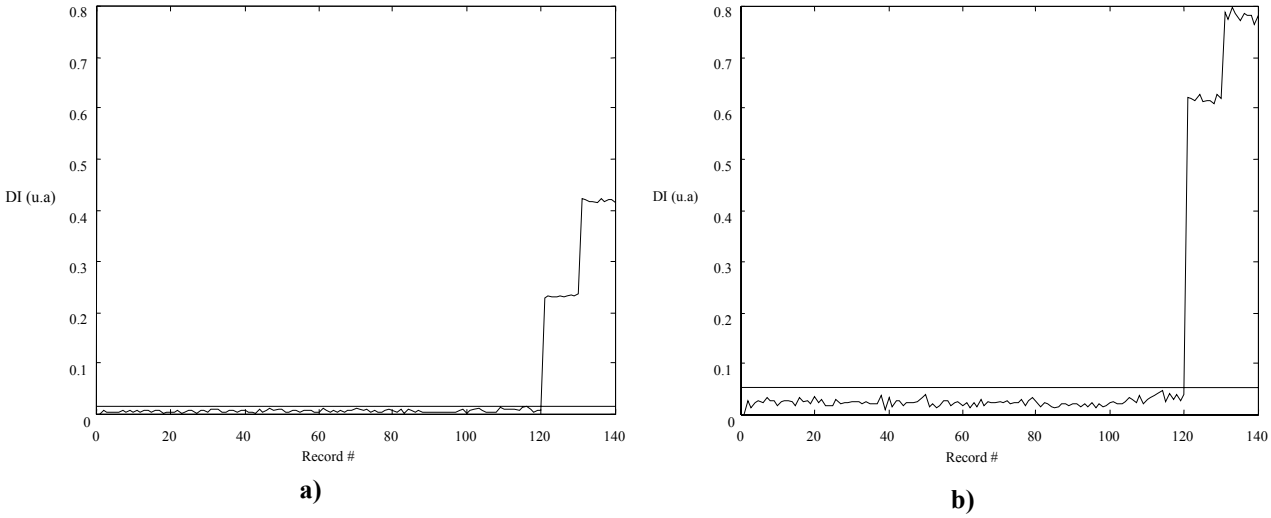

Fig. 6, Damage Index versus record number. a) S'_0 contribution, b) A'_0 contribution

In Fig. 6a the damage index is calculated in a time window corresponding to the arrival time of the S'_0 mode at the beginning of the measured waveform. The 100 reference signatures lead to a *DI* very close to zero. Then the 20 following signatures corresponding to two non damaging impacts also give a *DI* very similar. The threshold indicated by a horizontal line denotes 5 times the standard deviation of the reference set distribution. For the signatures corresponding to the 3rd impact the index raises to about 25 % and finally for the last 8 joules impact, the *DI* reaches 42 %. The non damaging impacts give results very similar to the reference set when the damaging impacts are clearly discriminated by two very different values of the index.

In Fig. 6b the damage index is calculated in a time window corresponding to the arrival time of the A'_0 mode. Once again, the 100 reference signatures and the 20 following signatures give almost the same *DI*. The A'_0 mode seem to be more sensitive to the presence of the delaminations since *DI* is about 62% for the 3rd impact and 78 % for the last one.

Our aim here is to simulate the interaction of guided waves with realistic damages. In the following, we introduced a sequence of delaminations of increasing length with depth in the CFRP plate described earlier. The delaminations are realized by introducing very thin elements of negligible elastic properties with respect to those of the constitutive plies. In accordance with literature and with our experimental observations, delaminations have been introduced at the interfaces between cross plies only. The first delamination localized under the impacted surface is 3.5 mm long and the deeper one is 42 mm long.

Fig. 8 shows a snapshot of the calculated out of plane displacement field u_3 associated to the propagation of a compressional (symmetrical-like) S'_0 guided wave, at a time t = 51.3 µs after the beginning of the wave excitation at the left edge of the plate. The wave is introduced in the FEM model by applying the S'_0 out of plane and in plane displacement fields profiles, calculated analytically, at a frequency-thickness product *fd* = 0.9 MHz.mm, for the sane CFRP plate,. The time dependency of these fields is a Hanning windowed, five periods tone-burts of 150 kHz.

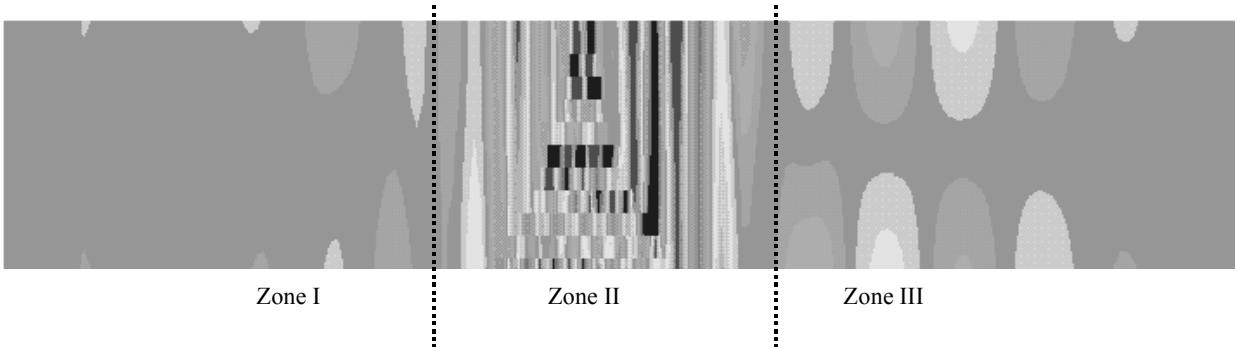

Fig. 7, Snapshot at t = 51.3 µs, of the out of plane displacement field u_3 du to the interaction of a compressional S'_0 mode with a conical delamination in a CFRP plate. (vertical scale magnified 10 times)

In Fig. 7, the guided S'_0 mode has yet been partially reflected and transmitted by the delamination located in Zone II. The calculated field in Zone I, is almost identical to the one obtained in the sane case. In Zone II, it can be observed some kind of mode conversion. The observed periodicity of the displacement field is much smaller (≈ 11 mm) than that of the S'_0 mode, but very close to the A'_0 mode theoretical wavelength ($\lambda \approx 7$ mm). Moreover the out of plane displacement field profile exhibits the typical symmetry with respect to the medium plane of the plate for a flexural mode. In Zone III, the displacement field profile is again typical of a compressional wave and exhibits the same wavelength as the incident mode.
So the calculated waveform on a point located 5 mm before the right edge of the plate shows a first echo which amplitude is lower than the first echo observed in the sane plate, followed by a second one of higher amplitude. The first echo can be ascribed to S'_0 mode while the second one is due to the arrival of the converted A'_0 mode. By windowing the waveform, it is possible to isolate the S'_0 contribution and to calculate the damage index *DI*, just as it has been done for the experimental measurement. We found *DI* = 47 %. This value is in really good agreement with the experimental one.
For comparison purposes, the same approach has been applied to an A'_0 mode interacting with the same defect in the same damaged plate. No mode conversion is observed when the A'_0 mode interacts with the damage. The main feature is that, compared to the sane plate, a huge decrease in the A'_0 mode amplitude is observed. The calculated waveform at the right edge of the plate allows the damage index to be calculated. It is evaluated to be about 76 %.
Then, despite no conversion mode occurs, it seems that this mode sensitivity to the conical delamination is better than that of the compressional one.

4.PASSIVE DAMAGE DETECTION IN COMPOSITE STRUCTURES

Since previous techniques use bonded or embedded piezoelectric sensors, these latter can be used as Acoustic Emission sensors and the recorded signals processed according to AE methodology. AE is an efficient method to monitor, in real time, damage growth in both structural components and laboratory specimens [7]. In loaded materials, the strain-energy release due to microstructural changes results in stress-wave propagation. In the case of composite materials, many mechanisms have been confirmed as AE [8,9,10] sources including matrix cracking, fibre-matrix interface debonding, fibre fracture and delamination..
In the following example, acoustic Emission (AE) was used to discriminate in real time the different types of damage occurring in a fibrous composite under mechanical load. For that purpose, we worked on polyester and glass/polyester unidirectional specimens, subjected to tensile loading within different configurations, awaiting preferential damage modes in the material. Three types of samples were used in this study: pure resin, 45° and 90° off-axis unidirectional samples. Each of these samples were chosen to support preferentially particular damage modes during tests: matrix fracture for resin samples, mainly matrix fracture with some decohesions for 90° off-axis, mainly decohesion with some matrix fracture for 45° off-

axis. Acoustic emission measurements were achieved by the use of two resonant micro80 PAC sensors, applied on the faces of the samples during testing.
Tensile tests on pure resin samples generated few AE activity. All AE waves detected can be considered as burst type signal which implies that the AE waves were generated during dynamic and discontinuous micro-fracture process in the sample. Signals appearing during the main part of the tests were associated to the nucleation and growth of vacuoles inside the resin i.e. matrix microcrack formation. From the test on resin samples, the acoustic signature of matrix fracture was determined: slowly rising waveform and low amplitude.
The amplitudes of the collected signals recorded during tests on unidirectional samples loaded in the transverse direction to fibres (90° off-axis) are mainly distributed in two zones (Fig. 8). About 70% of them have amplitudes in the range of 50 to 70 dB, with waveforms similar to those observed in the tests on pure resin ; we will refer these signals as “A-type” (Fig. 8, lower left). The 30% left signals have amplitudes in the range of 70 to 90 dB and waveforms quite different from A-type signals, with shorter decay time and higher energies. These signals will be referred as “B-type” (Fig. 8, lower right). The definition of the signal amplitude ranges is somewhat arbitrary. Nevertheless, such simple arbitrary guidelines can appear to be useful.

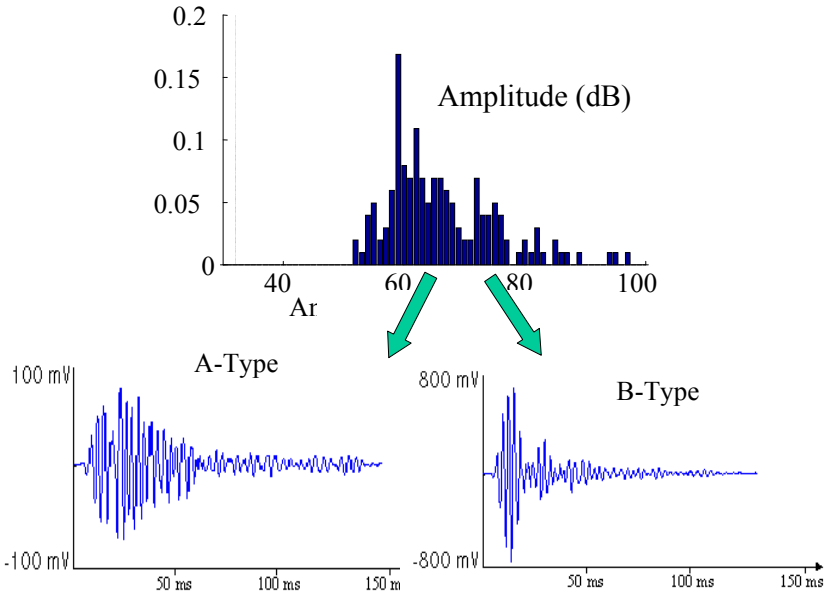

Fig. 8, Amplitude distribution and typical waveforms of signals from tensile tests on 90° samples

The similarities in waveforms found between A-type signals in 90° off-axis tests and signals from pure resin tests denotes that the source mechanism is the same in both cases, i.e. matrix fracture. In agreement with the fact that mode I cracking is the main fracture mode for this kind of sample. B-type signals (amplitudes between 70 and 90 dB) are detected only during the second half of the test as can be seen in Fig. 8, whereas the activity of A-type seems quite continuous. So, A-type and B-type seem to correspond to different mechanisms inside the material. B-type though must have another mechanical origin, occurring after certain matrix damage level has been attained.
The same test has been carried out for samples in the 45° direction to fibres. A-type and B-type signals can be observed in the same amplitude zones as previously and with very close parameters and waveforms. However, B-type signals are much more numerous than A-type in these tests (80%). The main expected damage mode in these types of tests, considering that 45° is the direction in which shear stress is maximum along the direction of fibres [11], is fibre/matrix decohesion. So the source of B-type signals might correspond to decohesion.

This is also consistent with their presence in the 90° tests, appearing after A-type, when matrix fracture surrounds the fibres. The fact that the fibre/matrix decohesions are dominant in the 45° tests was confirmed by SEM (Scanning Electronic Microscopy) observations.
The previous results are quite important in the goal of damage mechanism identification. It could be very interesting to find a method able to separate automatically A-type and B-type signals. For this purpose, a neural network approach was implemented. Such techniques have demonstrated their capabilities in functionally modelling processes involving many variables [12]. More precisely, a Kohonen self-organising feature map [10] was used to organise feature vectors into clusters so that points within one cluster are more similar to each others than vectors belonging to other clusters. The inputs were six AE features taken from the signals. The network response clearly exhibits two main clusters (Fig. 9), corresponding to the two types of signals previously observed.

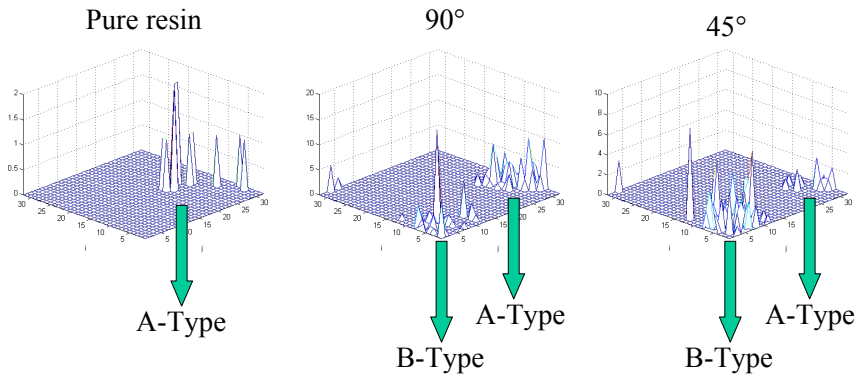

Fig. 9, Activations of the Kohonen map for the three types of tensile tests

The Kohonen map could then be used to compute the chronology of appearance of A-type or B-type signals during tests, as an indicator of the damaging kinetics of each damaging mechanisms. Interpretation of clustering results on a macroscopic level is performed by plotting the cumulative events of each class versus load. An example is given in Fig. 10 for two tests at 45° and 90° from fibres. It indicates a typical evolution of AE events, for the discriminated source mechanisms. For the 90° sample it is observed that the two classes exhibit similar activity trends. The fraction of A-type signals for the 90° sample increased more than for the 45° sample, from the beginning to the end of deformation. On the contrary, a larger fraction of B-type signal was detected for the 45° than for which. decohesion is the dominant damage mechanism. Let us also note that the number of B-type signals associated with decohesion, greatly increases at the end of tests, causing the final failure of the material.

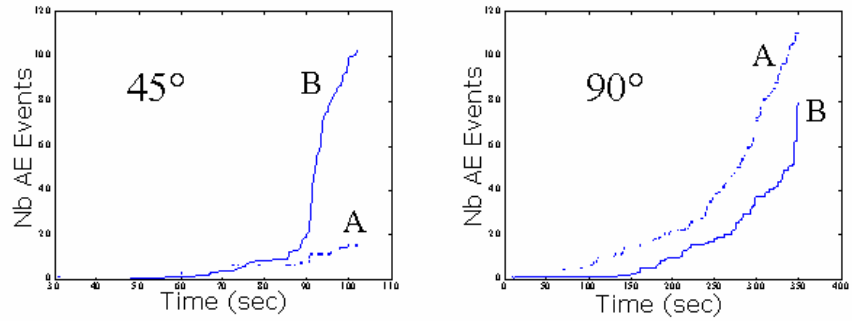

Fig. 10, AE activity evolutions of A-type and B-type during tests

5. CONCLUSIONS

Three possible implementation of the so called piezoelectric insert method have been illustrated on the basis of experimental results.

The same set of piezoelectric elements can be utilised for aging monitoring, for damage detection, location and identification and finally to record the AE activity of the structure under test. In the latter case, a neural network method allows the identification of the damage mechanisms.

This multifunctional character of the piezoelectric insert is quite relevant in the perspective of on-line health monitoring of aeronautical structures. Actually the use of the same set of sensors to perform at least three kind of measurement reduces the weight of the monitoring system and hence simplifies the maintenance process.

In the objective of the lifetime improvement of a structure, the piezoelectric sensor could also be used to perform an active or semi-passive vibration control.

REFERENCES

1 **GIURGIUTIU V.,** "Embedded Utrasonic NDE with Piezoelectric Wafer Sensors" RS-I2M - 3/2003 Ultrasonic Methods, pp 149 to 180.

2 **PERRISSIN-FABERT I., JAYET Y**., "Simulated and experimental study of the electric impedance of a piezoelectric element in a viscoelastic medium", Ultrasonics, Vol. 32,N° 2, pp. 107-112, 1994

3 **SAINT-PIERRE N., JAYET Y., GUY P., J. C. BABOUX J.C.**, "Ultrasonic evaluation of dispersive polymers by the piezoelectric embedded element method: modeling and experimental validation", Ultrasonics, Vol. 36, pp. 783-788, 1998

4 **MONNIER T, JAYET Y, GUY P, BABOUX JC,** The piezoelectric implant method: implementation and practical applications, J. of Smart Mater. Struct., vol.9, n°3, 2000, pp.267-272

5 **T. MONNIER, Y. JAYET, P. GUY, J.C. BABOUX, and P.F. GOBIN**, " Non destructive evaluation in composite structures using embedded piezoelectric sensors", Pr9oceedings of the 10th International Conference on Adaptive Structures and Technologies (ICAST '99), pp. 577-584, Paris, 1999

6 **Kronig R, Kramers H. A.,** Absorption and dispersion in X-ray spectra, Z. Phys., 48,1928, 174-187

7 **GODIN N., R'MILI M., MERLE P.and BABOUX J.C.**, Comptes Rendus des 11^{e} Journées Nationales sur les Composites (JNC11), Arcachon, 18-20 Novembre 1998.

8 **BARRÉ, S., BENZEGGAGH, M.-L.,** Comp. Science Tech.; **52,** pp. 369-376, 1994.

9 **ELY T. M., HILL E. K**, Materials Evaluation, pp.288-294, 1995.

10 **HUGUET S., GODIN N., GAERTNER R., SALMON L., DVILLARD D**., ECCM-9, Brighton UK, 4-7 Juin 2000.

11 **GAY, D.** (1991) Matériaux composites (3e ed.) Hermes, Paris

12 **FISHER M. E., HILL E. V. K**., Materials Evaluation, pp 1395, 1998